THE JOURNAL OF BIOLOGICAL CHEMISTRY VOL. 281, NO. 4, pp. 2249–2256, January 27, 2006

Structure of *Chlorobium tepidum* Sepiapterin Reductase Complex Reveals the Novel Substrate Binding Mode for Stereospecific Production of L-*threo*-Tetrahydrobiopterin*

Received for publication, August 24, 2005, and in revised form, November 17, 2005 Published, JBC Papers in Press, November 24, 2005, DOI 10.1074/jbc.M509343200

Supangat Supangat[‡§], Kyung Hye Seo[‡§], Yong Kee Choi[¶], Young Shik Park[¶], Daeyoung Son[‡§‖], Chang-deok Han[‡§‖], and Kon Ho Lee[‡§‖1]

From the [‡]Division of Applied Life Science, [§]Environmental Biotechnology National Core Research Center, and [‖]Plant Molecular Biology and Biotechnology Research Center, Gyeongsang National University, Jinju 660-701, Korea and [¶]School of Biotechnology and Biomedical Science, Inje University, Kimhae 621-749, Korea

Sepiapterin reductase (SR) is involved in the last step of tetrahydrobiopterin (BH_4) biosynthesis by reducing the di-keto group of 6-pyruvoyl tetrahydropterin. *Chlorobium tepidum* SR (cSR) generates a distinct BH_4 product, L-*threo*-BH_4 (6*R*-(1′*S*,2′*S*)-5,6,7,8-BH_4), whereas animal enzymes produce L-*erythro*-BH_4 (6*R*-(1′*R*,2′*S*)-5,6,7,8-BH_4) although it has high amino acid sequence similarities to the other animal enzymes. To elucidate the structural basis for the different reaction stereospecificities, we have determined the three-dimensional structures of cSR alone and complexed with NADP and sepiapterin at 2.1 and 1.7 Å resolution, respectively. The overall folding of the cSR, the binding site for the cofactor NADP(H), and the positions of active site residues were quite similar to the mouse and the human SR. However, significant differences were found in the substrate binding region of the cSR. In comparison to the mouse SR complex, the sepiapterin in the cSR is rotated about 180° around the active site and bound between two aromatic side chains of Trp-196 and Phe-99 so that its pterin ring is shifted to the opposite side, but its side chain position is not changed. The swiveled sepiapterin binding results in the conversion of the side chain configuration, exposing the opposite face for hydride transfer from NADPH. The different sepiapterin binding mode within the conserved catalytic architecture presents a novel strategy of switching the reaction stereospecificities in the same protein fold.

Sepiapterin reductase (SR)[2]; EC 1.1.1.153) catalyzes the last step of the *de novo* synthesis of tetrahydrobiopterin (BH_4) from GTP. BH_4 is a well known essential cofactor for aromatic amino acid hydroxylases (1) and nitric-oxide synthase (2) in humans and other higher organisms (3, 4). BH_4 deficiency in human results in severe neurological disorders like atypical phenylketonuria and monoamine neurotransmitter deficiency and is also implicated in Parkinson disease, Alzheimer disease, and depression (3, 5).

The pathway of the *de novo* biosynthesis of BH_4 from GTP involves only three enzymes, GTP cyclohydrolase I (EC 3.5.4.16), 6-pyruvoyltetrahydropterin (PPH_4) synthase (EC 4.2.3.12), and SR. SR catalyzes NADPH-dependent reduction of the di-keto group in the C6 side chain of PPH_4 to BH_4 (6) (Fig. 1). Biochemical and crystallographic analyses of murine SR suggest that SR has both reductase and isomerase activities; SR reduces first the C1′ carbonyl group and subsequently catalyzes an isomerization reaction shifting the C2′ carbonyl group to the C1′ position and then the second reduction of the carbonyl group to produce L-*erythro*-BH_4 (7, 8). Although SR is the only enzyme completing the step alone, other enzymes such as aldose reductase or carbonyl reductase also participate in the terminal step of BH_4 synthesis (9, 10). Aldose reductase catalyzes C2′-specific reduction of PPH_4 to produce 1′-oxo-2′-hydroxytetrahydropterin, which is then oxidized nonenzymatically to sepiapterin (6-lactoyl-dihydropterin) (10, 11). Sepiapterin is catalyzed *in vivo* by SR to 7,8-dihydrobiopterin, which is further reduced to BH_4 by dihydrofolate reductase, constituting an alternative pathway of BH_4 synthesis (10, 11).

Although L-*erythro*-BH_4 (6*R*-(1′*R*,2′*S*)-5,6,7,8-BH_4) is common in nature, other stereoisomers such as D-*threo*-BH_4 (6*R*-(1′*R*,2′*R*)) and L-*threo*-BH_4 (6*R*-(1′*S*,2′*S*)) are also found (12). D-*threo*-Form (dictyopterin) was isolated from *Dictyostelium* (12), and L-*threo* stereoisomer was isolated from *Chlorobium tepidum* as a glycoside (tepidopterin, L-*threo*-BH_4-N-acetylglucosamine) (13). It was shown that *C. tepidum* SR (cSR) catalyzes the reduction of not only sepiapterin to L-*threo*-H_2-biopterin (14) but also PPH_4 to L-*threo*-BH_4 (15). In contrast, D-*threo*-BH_4 was not produced by SR alone but by a collaborative work of SR and aldose reductase-like protein in *Dictyostelium* (16, 17).

cSR has high protein sequence similarities (~43%) with mouse SR (mSR) (PDB code 1SEP) and human SR (hSR)[3] (PDB code 1Z6Z) and is predicted to share the same fold as the homologous mSR (8) (Fig. 2). It was, therefore, a question how the structurally similar enzymes catalyze the synthesis of different isomeric forms of BH_4. Thus, we have determined the crystal structures of cSR alone and in complex with NADP and sepiapterin at 2.1 and 1.7 Å of resolution, respectively. The overall structure of cSR is quite similar to that of mSR. However, significant structural differences are observed in the substrate binding site of the two enzymes. Here, we report a novel ligand binding mode that determines the stereospecific catalysis of cSR in the production of L-*threo*-BH_4.

* This work was supported in part by 21C Frontier Functional Proteomics Project Grant FPR05B2-212 (to K. H. L.), Environmental Biotechnology National Core Research Center Grant R15-2003-002-01001-0 (to K. H. L.), Korea Science and Engineering Foundation Grant R05-2003-000-11206-0 (to Y. S. P.), Crop Functional Genomics Center of the 21st Century Frontier Research Program Grant CG1513 (to C.-d. H.), and by the BK21 program (to S. S. and K. H. S.). The costs of publication of this article were defrayed in part by the payment of page charges. This article must therefore be hereby marked "*advertisement*" in accordance with 18 U.S.C. Section 1734 solely to indicate this fact.

The atomic coordinates and structure factors (code 2BD0) have been deposited in the Protein Data Bank, Research Collaboratory for Structural Bioinformatics, Rutgers University, New Brunswick, NJ (http://www.rcsb.org/).

[1] To whom correspondence should be addressed. Tel.: 82-55-7516257; Fax: 82-55-759-9363; E-mail: lkh@gsnu.ac.kr.

[2] The abbreviations used are: SR, sepiapterin reductase; cSR, *C. tepidum* SR; mSR, mouse SR; hSR, human SR; BH_4, tetrahydrobiopterin; PDB, Protein Data Bank; PPH_4, 6-pyruvoyltetrahydropterin; SeMet, selenomethionine.

[3] E. Ugochukwa, K. Kavanagh, S. Ng, C. Arrowsmith, A. Edward, M. Sundstrom, F. von Delf, and U. Oppermann, unpublished material.

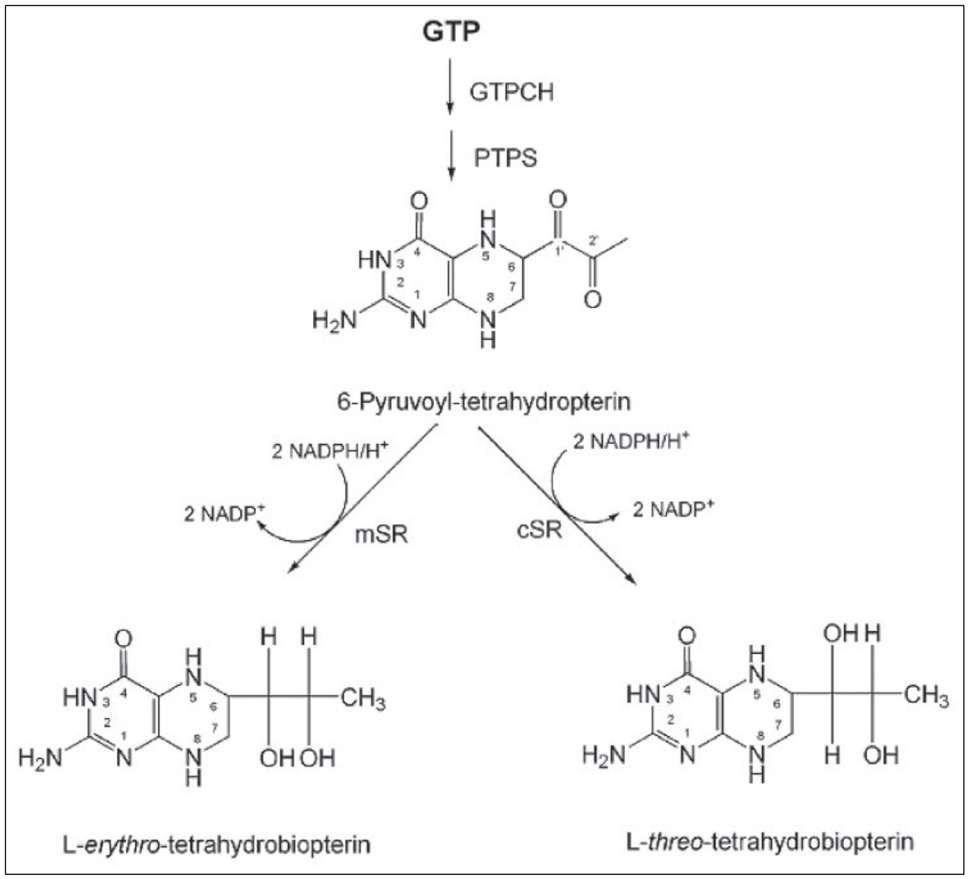

FIGURE 1. **The biosynthesis of tetrahydrobiopterin isomers.** At the terminal step of BH_4 synthesis, SR catalyzes PPH_4 via two step reductions and isomerization. cSR produces L-*threo*-6*R*-(1′*S*,2′*S*)-5,6,7,8-BH_4, whereas mSR produces L-*erythro*-6*R*-(1′*R*,2′*S*)-5,6,7,8-BH_4. *GTPCH*, GTP cyclohydrolase I; *PTPS*, 6-pyruvoyl-tetrahydropterin synthase.

EXPERIMENTAL PROCEDURES

Cloning, Expression, and Purification—The cSR was cloned, expressed, and purified following the protocols described previously (18). Briefly, cSRs were cloned into pET-28b and transformed into *Escherichia coli* strain BL21(DE3) for free cSR and B834(DE3)PLysS for selenomethionine (SeMet) derivative, respectively. The soluble protein was purified by nickel-agarose affinity, anion exchange, and gel filtration chromatography. The protein was concentrated to 10 mg/ml in 20 mM Tris-HCl, pH 8.0.

Crystallization and Data Collection—Free cSR and the SeMet-derivative proteins of cSR were crystallized following the protocols described previously (18). To prepare crystals of cSR-NADP-sepiapterin complex, protein was mixed with NADP and sepiapterin to final concentrations of 10 mM and incubated for 3 h before set-up. Crystals of free, SeMet-derivative protein and cSR-NADP-sepiapterin complex were obtained by hanging drop vapor diffusion method at 18 °C in a drop containing 4 μl of protein solution and 1 μl of a mixture of 4 μl of reservoir solution (0.2 M $MgCl_2$, 0.1 M Tris-HCl, pH 8.5, 34% polyethylene glycol 400) and 1 μl of additive (1 M guanidine hydrochloride).

X-ray diffraction data for free cSR and cSR-NADP-sepiapterin complex were collected from a single crystal to 2.1- and 1.7-Å resolution using x-ray of wavelength 1.1273 Å and a Bruker CCD detector at station 6B of the Pohang Accelerator Laboratory, Pohang, Republic of Korea, respectively. Diffraction data for SeMet derivative was collected from a single crystal to 2.1 Å of resolution at station 6A at the Photon Factory at the High Energy Accelerator Research Organization, Tsukuba, Japan. All diffraction images were indexed, integrated, and scaled using the HKL2000 suite (19). Both free and SeMet-derivative crystals are in space group R32, whereas the cSR-NADP-sepiapterin complex is in space group $P2_12_12_1$. Data collection statistics are presented in Table 1.

Structure Determination and Refinement—The structure of cSR was determined by a multiple wavelength anomalous diffraction experiment using the SeMet derivative (20). Attempts to solve the structure by molecular replacement using the program AMoRe (21) with the mSR as a search model have given no useful solutions. Diffraction was recorded at peak, inflection, and high energy remote points for multiple wavelength anomalous diffraction phasing. 33 selenium sites were located, and phases were calculated using SOLVE/RESOLVE (22). The atomic model was built into the electron density with the program O (23). The structure refinement was carried out with the program CNS (24). The stereochemistry of the structure was checked by PROCHECK (25). For free cSR, in the Ramachandran plot, 88.3% of all the residues are in most favored region, and for cSR-NADP-sepiapterin complex, 92.1% of all the residues are in most favored region. Figures were prepared using PyMOL (26). The statistics of the structure refinement are presented in Table 1.

RESULTS AND DISCUSSION

Structure Determination—The crystal structure of the free enzyme of cSR was solved at 2.1 Å of resolution using the selenomethionyl multiple wavelength anomalous diffraction method. There are four molecules in the asymmetric unit of the crystal, and 33 of the expected 40 selenium positions were located from the anomalous difference data. The current atomic model has an *R* value of 20%, and most of the residues (91%) are in the most favored region of the Ramachandran plot (data not shown). The crystallographic data and refinement statistics are summarized in Table 1.

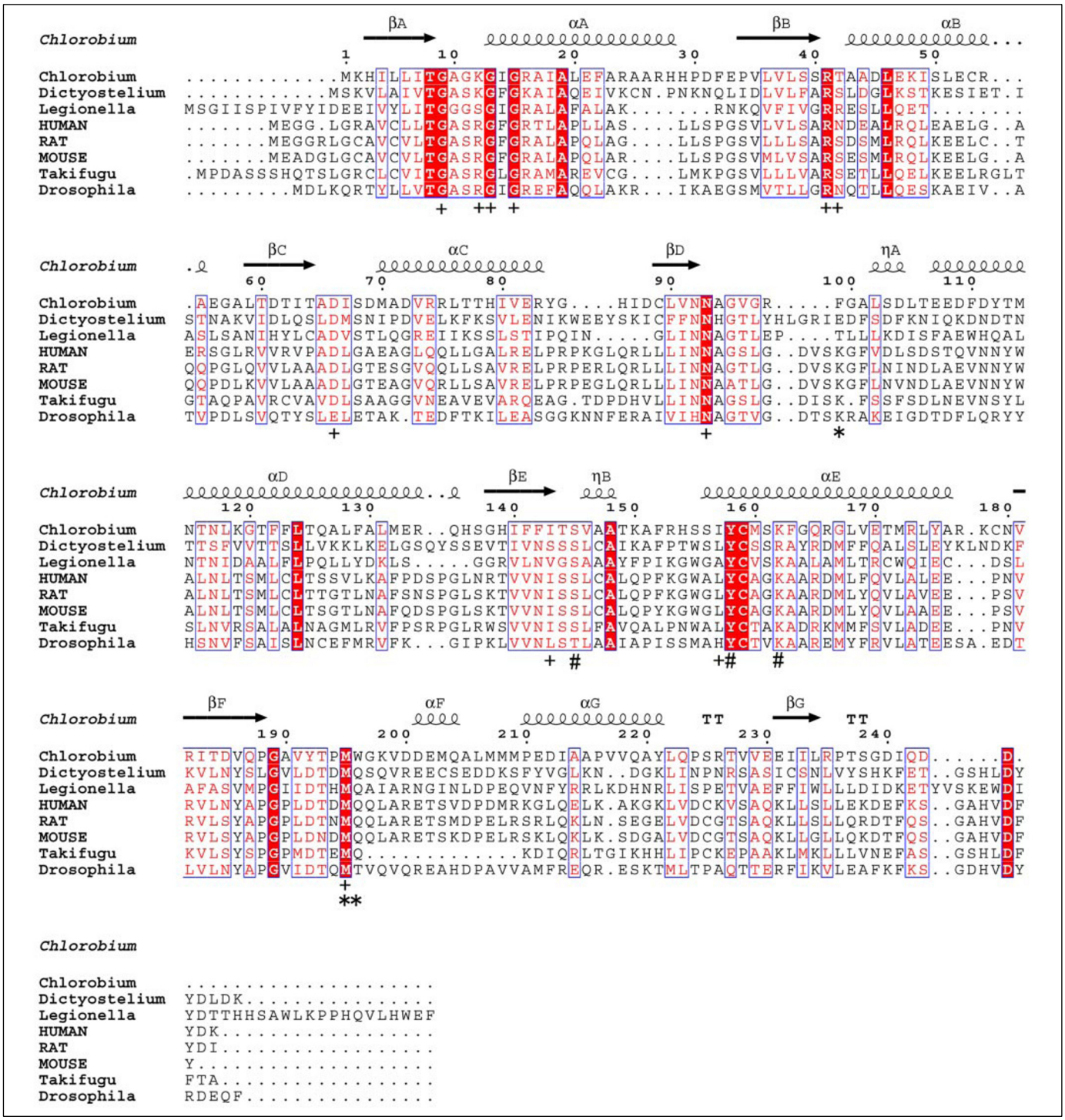

FIGURE 2. **Sequence alignment of SRs from *Chlorobium* and mammals.** The amino acid sequence alignment of SRs from *C. tepidum*, *Dictyostelium discoideum*, human, rat, mouse, *Takifugu rubripes*, and *Drosophila melanogaster* is shown. A *column* is framed in *red* when residues are identical and *boxed* when at least four of its residues (*red*) are homologues. Residues for cofactor binding are marked with a plus (+), central residues for substrate binding in the *Chlorobium* are marked with an *asterisk* (*), and catalytic triad residues are marked with a *number sign* (#). Correspondence between amino acid sequences and the secondary structure defined by DSSP (38) is given on *top* for *Chlorobium* SR; helices are shown as *coils*, and β-strands are shown as *arrows*. The alignment was done by ClustalX (39), and the figure was drawn with ESPript (27).

The structure of cSR in complex with NADP and sepiapterin has been determined at 1.7 Å of resolution (Table 1) from a co-crystal obtained from the mixture of protein, NADP, and sepiapterin. The complex was packed in space group $P2_12_12_1$ different from the free enzyme in space group R32. There are four molecules in the asymmetric unit and one NADP per molecule and one sepiapterin molecule modeled in the tetramer. The other three sepiapterin molecules have weak electron densities and are not included in the model. In both free enzyme and NADP-sepiapterin complex, the N-terminal hexahistidine tag and residue 1 are disordered. In addition, residues 194–203 of the free enzyme are disordered and not included in the atomic model. Also, residues 198–202 in the complex have weak electron densities for side chains and are modeled as alanines.

Overall Structure of cSR—In the cSR crystal structure, each monomer (244 residues) folds into a single domain α/β-structure. A seven-

TABLE 1
Crystallographic statistics

	Native		SeMet		NADP-Sepiapterin complex
Data statistics					
Space group	R32[a]		R32		$P2_12_12_1$
Unit cell (Å)	$a = 202.14$, $c = 210.02$		$a = 201.14$, $c = 210.18$		$a = 84.36$, $b = 97.48$, $c = 123.24$
No. of chains in AU	4 molecules		4 molecules		4 molecules
		Peak	Edge	Remote	
Wavelength (Å)	1.123	0.978	0.9793	0.9704	1.123
Resolution (Å)	50 = 2.15 (2.23–2.15)[b]		25 = 2.1 (2.18 = 2.1)		35 = 1.7 (1.76 = 1.7)
Completeness (%)	99.2 (98.5)	99.9 (99.7)	99.9 (99.7)	99.9 (99.7)	99.8 (93.8)
$R_{sym}(I)$[c] (%)	14.6[d] (89.7)	11.3 (60.2)	10.4 (64)	10.9 (66.7)	7.4 (51.9)
Redundancy	19	10.2	10.3	10.1	7
$\langle I/\sigma(I)\rangle$	7.0	11.1	11.0	11.6	19.3
Figure of merit			0.47/0.68[e]		
Refinement					
Protein atoms	7386				7955
Water molecules	284				369
R_{free}[f] (%)	23.8 (30.17)				21.3 (28.08)
R_{work}[f] (%)	21.9 (28.31)				20.0 (25.90)
Root mean square deviations					
Bond length (Å)	0.007				0.005
Bond angle (°)	1.26				1.29
Mean *B*-factors (Å^2)					
Protein	33				24
Water	33				28
NADP					22
Sepiapterin					47

[a] IIexagonal indexing with $\alpha = \beta = 90°$ and $\gamma = 120°$.
[b] Numbers in parentheses represent values in the highest resolution shell.
[c] $R_{sym}(I) = (\Sigma_{hkl}|I-\langle I\rangle|/\Sigma_{hkl}\langle I\rangle)$, where *hkl* are independent Miller indices.
[d] This value is a little higher because of high mosaicity of the data.
[e] As indicated by SOLVE/RESOLVE.
[f] $R_{free} = \Sigma_{hkl}|F_o - F_c|/\Sigma_{hkl}F_o$, where *hkl* is a free set; $R_{work} = \Sigma_{hkl}|F_o - F_c|/\Sigma_{hkl}F_o$, where *hkl* is a working set.

stranded parallel β-sheet in the center of the molecule is sandwiched by two layers of three α-helices (αA, αB, αF and αC, αD, αE), homologous to those found in other short chain dehydrogenase/reductase including mSR and hSR (8, 28, 29)[3] (Fig. 3*A*). The central six strands form a typical dinucleotide binding motif (29) composed of βαβ units. A Dali (30) search for structurally similar proteins showed that the cSR chain topology matches most closely other short chain dehydrogenase/reductases (PDB codes 1YBV, 1FDS, 1CYD, 1GZ6, 1E6W, 1OAA, 1BDB, 1E7W) with Z scores greater than 24. The overall folding of cSR is similar to mSR and hSR, sharing a common tertiary structure with an NADP(H) cofactor binding site and a conserved Y*XXX*LYS sequence motif with root mean square deviations of 0.90 and 1.16 Å to hSR and mSR among C^{α} atoms in the central β-sheet, respectively (calculated with lsqkab in CCP4 Suite) (21).

However, significant differences between cSR and mSR or hSR molecules were observed in the substrate binding region around the active site. The loop between βF and αF (residues Val-191 to Met-207; 17 amino acids) in cSR is much shorter than that in mSR (residues Leu-202 to Leu-232; 31 amino acids) and in hSR (residues Leu-198 to Leu-228; 30 amino acids) (Fig. 3*C*). Also, the residues in the loop between βF and αF show low sequence similarities among these enzymes. The residues at the C-terminal region from Arg-235 to Ile-241 in the cSR extend longer so that it covers up the side of the cavity that is open in the mSR and hSR (Fig. 3*C*). Therefore, the short loop and the long C-terminal extension in the cSR make changes in the shape and the size of the substrate binding cavity. These changes around the binding cavity may explain the different stereospecific catalysis of the enzyme.

Structure of the cSR Tetramer— cSR is a tetramer in the asymmetric unit of the crystal formed by two homodimers, although cSR exists as a homodimer in solution, confirmed by gel filtration and cross-linking experiment (data not shown). The four cSR molecules in the asymmetric unit have essentially the same conformation, with average root mean square distances of 0.21 Å between equivalent Cα atoms for the free enzyme and 0.27 Å for the NADP-sepiapterin complex (calculated with lsqkab for all Cα pairs). In the tetramer there are two different monomer-monomer interactions by the associations of two cSR monomers, each monomer contacting with two neighboring monomers in a head-to-tail fashion related by a noncrystallographic 2-fold axis (Fig. 3*B*). The interface between chain A and B is formed by a four-helix bundle consisting of helices αD and αE of each chain. A number of hydrophobic interactions are found in this interface area, involving Phe-110, Phe-122, Phe-123, and Phe-163 from each monomer together with a salt bridge between Asp-111 of monomer A and Lys-119 of monomer B. Another dimer interface is formed between chain A and C by contacts between strand βG and helix αF from each monomer. In this dimer the β-sheet of each monomer is connected by strand βG in an antiparallel manner to each other, forming a central 14-stranded β-sheet. There is an additional salt bridge at the interface formed between Asp-212 and Arg-226 of helix αF from each monomer. No interactions are found between chain A and D, leaving a hole in the center of the tetramer filled with many solvent molecules.

Active Site in cSR—In the cSR-NADP-sepiapterin complex structure, the active site can be identified from the positions of the bound NADP and sepiapterin (Fig. 4*B*). The pocket for substrate is located around at the C terminus formed by the three long loops between strand βD and helix αD, between βE and αE, and between βF and αF and also by a C-terminal extension of strand βG. The loop between βF and αF has two additional short helices αFG1 and αFG2 that are partially disordered in the absence of substrate (Fig. 3*A*). The substrate binding site is at the C-terminal end of the β-strands above the nicotinamide ring of the NADP. The active site cavity in the NADP-sepiapterin complex is formed by hydrophobic and polar residues Val-146, Ala-147, Phe-99, Arg-150, Phe-152, Ser-145, Tyr-158, Met-195, Arg-235, Asp-240, and Ile-241.

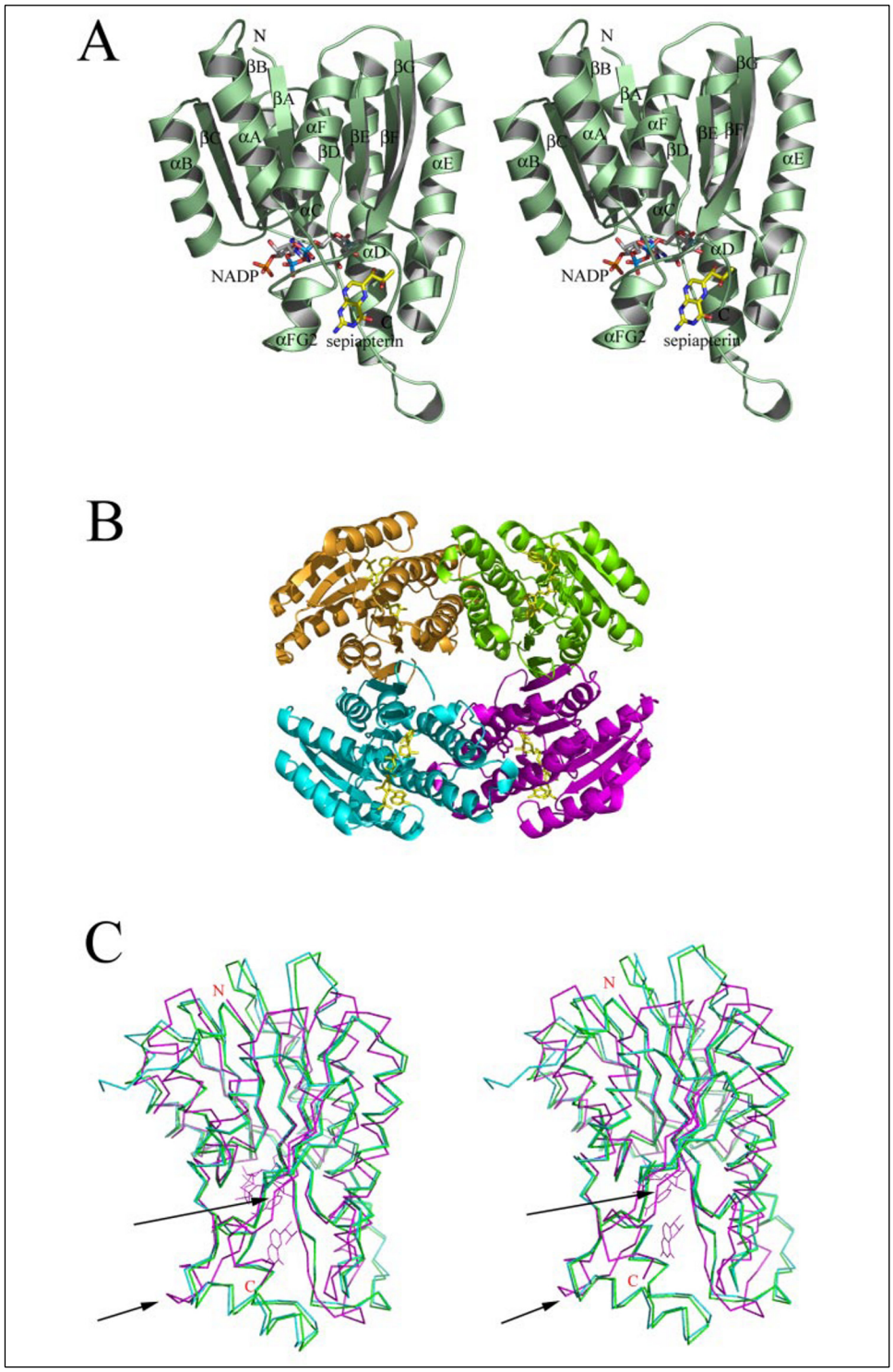

FIGURE 3. **Overall structure of cSR.** *A*, stereoview of ribbon representation of the cSR monomer. β-Strands and α-helices are labeled in alphabetical order from the N terminus. NADP (*gray*, carbon; *red*, oxygen; *blue*, nitrogen; *orange*, phosphate) and sepiapterin (*yellow*, carbon; *red*, oxygen; *blue*, nitrogen) are shown as *sticks*. *B*, *ribbon* representation of a cSR tetramer formed by two dimers in the asymmetric unit (chain A is in *orange*, B is in *green*, C is in *cyan*, and D is in *magenta*). There are two different dimer interfaces, one between the *orange* and *green* monomers and the other between the *orange* and *cyan* monomers. *C*, superposition of the SR monomers from *Chlorobium* (*magenta*), mouse (*green*; PDB code 1SEP) and human (*cyan*; PDB code 1Z6Z) with NADP (*magenta*) and sepiapterin (*magenta*) bound in the cSR. The largest differences from the three structures are marked with *arrows*.

Enzymes of the short chain dehydrogenase/reductase family contain a highly conserved Ser-Tyr-Lys triad at the active site (32). In the cSR crystal structures three residues forming a Ser-Tyr-Lys triad at the active site are well conserved as in other SRs (Fig. 4*C*). The tyrosine residue Tyr-158 is oriented for optimal hydride transfer from NADPH to the carbonyl functional group of the sepiapterin and plays a central role in the active site for the catalysis. The basic residue Lys-162, positioned close to Tyr-158, may stabilize the resulting tyrosinate. The Ser-145, which is located in hydrogen bond distance to the C1′-side chain oxygen, is also involved in proton transfer and stabilization for the carbonyl group (33) (Fig. 4*C*).

The substrate acceptor site in the cSR structure is different from that found in mSR (Fig. 4*C*). In the mSR-NADP-sepiapterin complex structure, the substrate binding site is located at the end of strands βD and βE between residues Leu-159 and Pro-199. However, the site is not accessible any more in the cSR structure for the substrate because it is occupied and blocked by the side chains of Val-146 and Arg-235. In addition, the strand βE shifted closer by 3.1 Å toward the βD strand from the

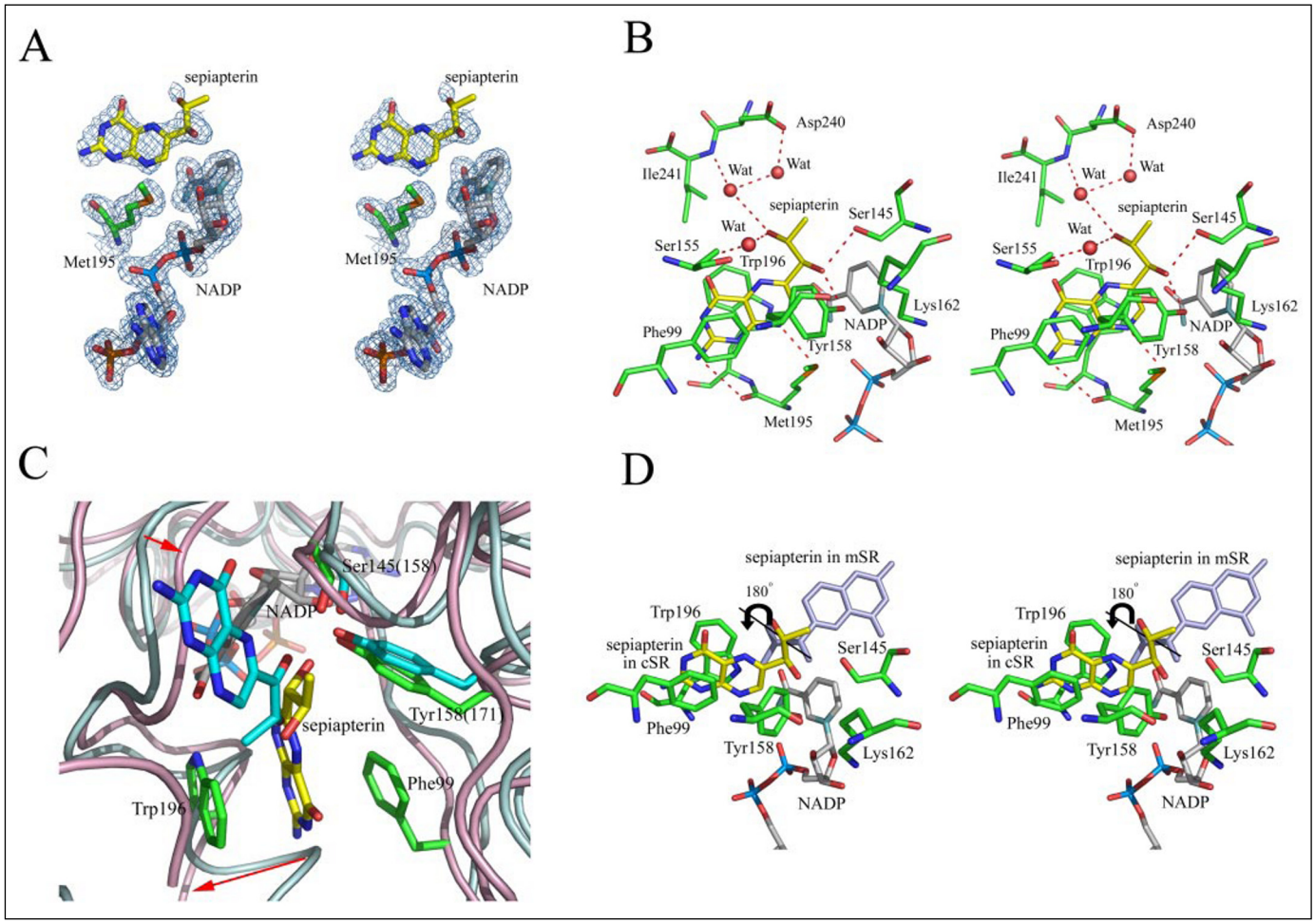

FIGURE 4. **The sepiapterin binding mode.** *A*, stereoview of the electron density of the sepiapterin, NADP, and Met-195. The electron density map ($2F_o - F_c$) contoured in 1σ of the sepiapterin (*yellow*, carbon; *red*, oxygen; *blue*, nitrogen), NADP (*gray*, carbon; *red*, oxygen; *blue*, nitrogen; *brown*, phosphate), and Met-195 (*green*, carbon; *red*, oxygen; *blue*, nitrogen; *orange*, sulfur) is shown in *blue*. *B*, stereographic diagram of the active site in the cSR complex. Sepiapterin, residues Phe-99, Ser-145, Ser155, Tyr-158, Lys-162, Met195, Trp-196, Asp-240, and Ile-241, and NADP are shown as *sticks*. Water (*Wat*) molecules are shown as *spheres* (*red*). Hydrogen bonds between sepiapterin and the residues are shown in *dashed lines* (*red*). *C*, *ribbon diagram* of superposition of the cSR (*pale magenta*) and mSR (*pale cyan*) at the active site. The sepiapterin in cSR and the sepiapterin in mSR (*cyan*, carbon; *red*, oxygen; *blue*, nitrogen) are shown as *sticks*. The central residues for substrate binding and catalysis are shown as *sticks*; that is, residues Phe-99, Tyr-158, Ser-145, and Trp-196 from cSR and residues Tyr-171 and Ser-158 from mSR (*cyan*, carbon; *red*, oxygen; *blue*, nitrogen). The shifts of loops in cSR from the positions in mSR are marked as *arrows* in *red*. Because of these shifts, sepiapterin in cSR cannot bind to the site in which sepiapterin in mSR is bound. *D*, stereographic diagram of substrate binding mode. Rotation of the sepiapterin is represented by the rotation axis, and the direction of the rotation is marked as an *arrow* in *black*. Sepiapterin in cSR, sepiapterin in mSR (*white blue*), NADP, and residues are shown as *sticks*.

position in the mSR structure, which leaves no space enough for the substrate binding around this region (Fig. 4*C*). As a result, the substrate binding site in the cSR has a 10-Å deep pocket shallower than a 15-Å deep pocket in the mSR and is open toward the C-terminal bottom of the molecule.

Conformational changes by substrate binding occur in the cSR structure as seen in a substrate binding loop in the structure of 7α-HSDH (31), although no changes were observed in the mSR structure. Without the substrate binding, the loop region of residues Val-191 to Met-207 in helices αFG1 and αFG2 is not defined well and has high temperature factors. Upon substrate binding, the side chains of residues 193–197 have clear electron densities, and the side chain of Trp-196 in the loop specifically interacts with the pterin moiety of the substrate (Fig. 3*C*).

NADP Binding Mode—In the cSR complex the cofactor NADP is well ordered and has well defined electron density. The bound NADP molecule has an extended conformation with the adenine ring in *anti* and the nicotinamide ring in *syn* conformations and binds at the C-terminal side of the parallel β-sheet in a similar way as seen in mSR (8). Both the ribose rings in the NADP have C^2-endo puckering conformations. Most of the residues in direct contact with the NADP in the cSR complex structure are conserved and occupy similar positions as in mSR, including a well conserved Arg-41 in the members of the short chain dehydrogenase/reductase family, which prefer NADP(H) (32) instead of NAD(H). The nicotinamide ring has its B-face oriented toward the substrate, allowing a B-face hydride transfer reaction.

Sepiapterin Binding Mode—The substrate, sepiapterin, is bound in the open pocket formed by the C terminus of strand βD, βE, and βF above the NADP nicotinamide ring. Sepiapterin has well defined electron density (Fig. 4*A*). In the active site the sepiapterin is bound by the pterin moiety stacked between the side chains of Phe-99 and Trp-196 with stacking distances of about 3.6 and 4.0 Å, respectively, and orients its side chain toward Tyr-158 OH and NADP C4′N (Fig. 4*B*). Hydrogen bonds formed between N1 and N2 of the pterin ring and the carbonyl oxygen of Met-195 and also between C2′-carbonyl and the side chains of Ser-155 and Asp-240, mediated by water molecules (Fig. 4*B*). Phe-99 and Trp-196 seem essential in determining the substrate binding specificities and keep the substrate by stacking its pterin moiety between their side chains. The distances between the C1′-carbonyl oxygen atom of the sepiapterin and Tyr-158 OH and the C4N′ are 2.56 and 3.58 Å, respectively.

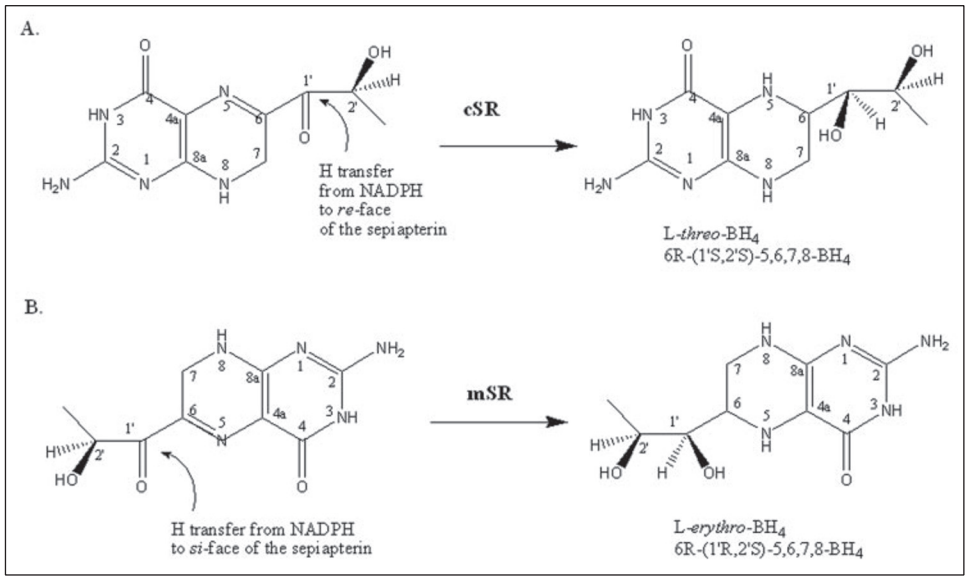

FIGURE 5. **Possible stereospecific hydride transfer in cSR.** The hydride transfer from NADPH to the sepiapterin bound in cSR (*A*) and mSR (*B*).

When compared with the mSR complex structure, the largest difference is observed in the position of the pterin ring of the sepiapterin bound in the cSR complex. The sepiapterin is rotated about 180° from the position in the mSR complex along the axis passing the C1′ carbon and perpendicular to the pterin ring in the active site (Fig. 4*D*). As a result, the sepiapterin is reversed so that its pterin ring is shifted to the entry of the active site from the sepiapterin position in the mSR complex. Therefore, the carbonyl oxygen atom of the pterin ring points up, away from the NADP, whereas the atom in the mSR points down toward the NADP (Fig. 4*D*). However, the coordination of the sepiapterin side chain in the cSR complex is not changed in this binding mode. The C1′ carbonyl oxygen atom is located close to the Tyr-158 OH and points toward Tyr-158 OH in the same way in the mSR complex. This different binding mode of the sepiapterin in the cSR structure causes the face conversion of the substrate toward the active site triad.

Catalytic Mechanism for M*-threo-BH_4*—SR is generally capable of catalyzing the NADPH-dependent reduction of both side-chain keto groups of PPH_4 to produce BH_4. cSR especially produces L-*threo*-BH_4 from PPH_4, whereas other SRs identified so far generate L-*erythro*-BH_4 (34, 35). The conserved positions of the sepiapterin side chain and the catalytic triad residues in the cSR complex strongly suggest that cSR follows the catalytic mechanism of the mSR; PPH_4 is catalyzed by two successive reductions of the C1′ carbonyl functions via isomerization (7, 8). cSR first reduces the C1′ carbonyl group in an NADPH-dependent manner to produce 1′-D-hydroxy-2′-oxopropyl-H_4-pterin and subsequently catalyzes an isomerization reaction, shifting the C2′ carbonyl group to the C1′ position via an endiol intermediate to produce 1′-oxo-2′-L-hydroxy-H_4-pterin; it then repeats the stereospecific reduction of the regenerated C1′ carbonyl group to produce L-*threo*-BH_4. From the crystal structure of the cSR complex, it is not known which amino acid residues are involved in internal rearrangement of the keto groups, but they are presumed to be conserved in cSR as in other SRs because the resulting 2′ carbons have identical configurations in both L-*erythro*- and L-*threo*-BH_4. The C1′ carbonyl is reduced by a stereospecific transfer of hydride ion from the exposed C4 of the nicotinamide and extraction of a proton from Tyr-158 by the negatively charged carbonyl oxygen. Lys-162 is located nearby Tyr-158 and Ser-145 and stabilizes the nicotinamide nucleoside moiety of the bound cofactor NADP(H).

The binding site for cofactor NADPH is open to the opposite side of the molecule. Therefore, the oxidized cofactor NADP after the first reduction may be exchanged to NADPH for the second reduction, whereas the substrate stays bound in the active site.

Stereospecific Production of M*-threo-BH_4*—The crystal structure of cSR complex reveals that the substrate binds around the active site in a different orientation from the mSR complex. The pterin ring of the sepiapterin in the cSR complex is rotated about 180° from the position of the sepiapterin in the mSR complex, but the side chain keeps the same position toward the active site residues (Fig. 4*C*). In this binding mode the face of the reaction for hydride transfer is converted; the C1′ carbon in the cSR is in a *si*-face toward NADP(H) C4′N, whereas it is in a *re*-face in the mSR complex. Therefore, after hydride transfer from NADPH, the C1′ carbon in the cSR complex is in *S* conformation, whereas the C1′ carbon in the mSR complex is in *R* conformation (Fig. 5). Thus, cSR is able to produce a L-*threo*-6*R*-(1′*S*,2′*S*)-5,6,7,8-BH_4 stereoisomer from the same substrate by changing the substrate binding orientation without any changes in the active site residues. This strategy of conserving the active site architecture seems to be highly reasonable in terms of protein evolution because any serious variations in the active site residues to accommodate different stereospecific catalysis might have been more detrimental to the protein than the small changes in the substrate binding site residues. The different reaction stereospecificities in the same protein fold was also observed in tropinone reductases (36), which catalyze the three-carbonyl group of tropinone to hydroxyl groups with different stereoisomeric configurations. In addition, the stereospecificities of tropinone reductase was reversed by substituting five amino acids at the substrate binding site (37). Although the structure of tropinone reductase complexed with its substrate has not been determined, it was suggested that the substrate of tropinone reductase binds in flip-over mode. cSR achieves the stereospecific production by altering the substrate binding site through the substrate rotation rather than the simple substrate flip-over modeled in the tropinone reductase. The swiveled substrate binding resulted from the shift of the binding site is so far a novel strategy to switch the reaction stereospecificities in the same protein fold.

Acknowledgments—We thank the staff at the Pohang Accelerator Laboratory beamline 6B, Korea and at the Photon Factory of the High Energy Accelerator Research Organization, Japan for help with the data collection. We also thank members of the Plant Molecular Biology & Biotechnology Research Center for assistance.

REFERENCES

1. Kaufman, S. (1993) *Annu. Rev. Nutr.* **13,** 261–286
2. Marletta, M. A. (1994) *Cell* **78,** 927–930
3. Thöny, B., Auerbach, G., and Blau, N. (2000) *Biochem. J.* **347,** 1–16
4. Werner-Felmayer, G., Golderer, G., and Werner, E. R. (2002) *Curr. Drug Metab.* **3,** 159–173
5. Blau, N., Bonafe, L., and Thöny, B. (2001) *Mol. Genet. Metab.* **74,** 172–185
6. Katoh, S., and Sueoka, T. (1987) *J. Biochem.* (*Tokyo*) **101,** 275–278
7. Katoh, S., and Sueoka, T. (1988) *J. Biochem.* (*Tokyo*) **103,** 286–289
8. Auerbach, G., Herrmann, A., Gutlich, M., Fischer, M., Jacob, U., Bacher, A., and Huber, R. (1997) *EMBO J.* **16,** 7219–7230
9. Milstien, S., and Kaufman, S. (1989) *Biochem. Biophys. Res. Commun.* **165,** 845–850
10. Park, Y. S., Heizmann, C. W., Wermuth, B., Levine, R. A., Steinerstauch, P., Guzman, J., and Blau, N. (1991) *Biochem. Biophys. Res. Commun.* **175,** 738–744
11. Bonafe, L., Thony, B., Penzien, J. M., Czarnecki, B., and Blau, N. (2001) *Am. J. Hum. Genet.* **69,** 269–277
12. Klein, R., Thiery, R., and Tatischeff, I. (1990) *Eur. J. Biochem.* **187,** 665–669
13. Cho, S. H., Na, J. U., Youn, H., Hwang, C. S., Lee, C. H., and Kang, S. O. (1998) *Biochim. Biophys. Acta* **1379,** 53–60
14. Cho, S. H., Na, J. U., Youn, H., Hwang, C. S., Lee, C. H., and Kang, S. O. (1999) *Biochem. J.* **340,** 497–503
15. Choi, Y. K., Jun, S. R., Cha, E. Y., Park, J. S., and Park, Y. S. (2005) *FEMS Microbiol. Lett.* **242,** 95–99
16. Kim, Y. A., Chung, H. J., Kim, Y. J., Choi, Y. K., Hwang, Y. K., Lee, S. W., and Park, Y. S. (2000) *Mol. Cell* **10,** 405–410
17. Choi, Y. K., Park, J. S., Kong, J. S., Morio, T., and Park, Y. S. (2005) *FEBS Lett.* **579,** 3085–3089
18. Supangat, S., Choi, Y. K., Young, S. P., Son, D., Han, C. D., and Lee, K. H. (2005) *Acta Crystallogr. F* **61,** 202–204
19. Otwinowski, Z., and Minor, W. (1997) *Methods Enzymol.* **276,** 307–326
20. Hendrickson, W. A. (1991) *Science* **254,** 51–58
21. CCP4 (1994) *Acta Crystallogr. D* **50,** 760–763
22. Terwilliger, T. C., and Berendzen, J. (1999) *Acta Crystallogr. D* **55,** 1872–1877
23. Jones, T. A., Zou, J. Y., Cowan, S. W., and Kjeldgaard, M. (1991) *Acta Crystallogr. A* **47,** 110–119
24. Brünger, A. T., Adams, P. D., Clore, G. M., DeLano, W. L., Gros, P., Grosse-Kunstleve, R. W., Jiang, J. S., Kuszewski, J., Nilges, M., Pannu, N. S., Read, R. J., Rice, L. M., Simonson, T., and Warren, G. L. (1998) *Acta Crystallogr. D* **54**, 905–921
25. Laskowski, R. A., MacArthur, M. W., Moss, D. S., and Thornton, J. M. (1993) *J. Appl. Crystallogr.* **26,** 283–291
26. DeLano, W. L. (2001) *The pyMol Molecular Graphics System*, DeLano Scientific, San Carlos, CA
27. Gouet, P., Courcelle, E., Stuart, D. I., and Metoz, F. (1999) *Bioinformatics* **15,** 305–308
28. Ghosh, D., Wawrzak, Z., Weeks, C. M., Duax, W. L., and Erman, M. (1994) *Structure* **2,** 629–640
29. Rossmann, M. G., Liljas, A., Bränden, C.-I., and Banaszak, L. J. (1975) *The Enzymes*, pp. 61–102, Academic Press, Inc., New York
30. Holm, L., and Sander, C. (1995) *Trends Biochem. Sci.* **20,** 478–480
31. Tanaka, N., Nonaka, T., Nakanishi, M., Deyashiki, Y., Hara, A., and Mitsui, Y. (1996) *Structure* **4,** 33–45
32. Jörnvall, H., Persson, B., Krook, M., Atrian, S., Gonzalez-Duarte, R., Jeffery, J., and Ghosh, D. (1995) *Biochemistry* **34,** 6003–6013
33. Fujimoto, K., Hara, M., Yamada, H., Sakurai, M., Inaba, A., Tomomura, A., and Katoh, S. (2001) *Chem. Biol. Interact.* **130–132,** 825–832
34. Katoh, S., and Sueoka, T. (1984) *Biochem. Biophys. Res. Commun.* **118,** 859–866
35. Smith, G. K. (1987) *Arch. Biochem. Biophys.* **255,** 254–266
36. Nakajima, K., Yamashita, A., Akama, H., Nakatsu, T., Kato, H., Hashimoto, T., Oda, J., and Yamada, Y. (1998) *Proc. Natl. Acad. Sci. U. S. A.* **95,** 4876–4881
37. Nakajima, K., Kato, H., Oda, J., Yamada, Y., and Hashimoto, T. (1999) *J. Biol. Chem.* **274,** 16563–16568
38. Kabsch, W., and Sander, C. (1983) *Biopolymers* **22,** 2577–2637
39. Thompson, J. D., Gibson, T. J., Plewniak, F., Jeanmougin, F., and Higgins, D. G. (1997) *Nucleic Acids Res.* **25,** 4876–4882